Available online at www.sciencedirect.com
SCIENCE DIRECT®
Coordination Chemistry Reviews 238–239 (2003) 127–141
COORDINATION CHEMISTRY REVIEWS
www.elsevier.com/locate/ccr

Theory of electroabsorption spectroscopy in poly-nuclear Ru complexes

Alessandro Ferretti *

Istituto per i Processi Chimico-Fisici del CNR, Area della Ricerca di Pisa, Via G. Moruzzi 1, I-56124 Pisa, Italy

Received 5 March 2002; accepted 6 January 2003

Contents

Abstract

Electroabsorption spectroscopy is a powerful experimental technique for the study of the charge transfer states of inorganic molecules. From the difference between the near IR–vis spectra, with and without the application of an electric field, it is possible to extract the value of the variation of dipole moment and polarizability in the transition between the ground and the first few low lying excited states of mono- and poly-nuclear ligand-bridged transition metal complexes. How these quantities and the difference spectra themselves can be obtained by theoretical methods is the subject of the present review. After a brief outline of the experiments and of the background theory which is used to obtain the relevant parameters from the measured difference spectra, the two-state electronic model and its connections to electroabsorption spectra are discussed. The inclusion of selected nuclear degrees of freedom and electronic correlation effects in the computation of line-shape profiles are then examined. This is done within the framework of simple model Hamiltonians which may be applied to the study of the optical properties of the various members of a class of Ru-ligand poly-nuclear complexes, as well as by the use of extensive ab initio multireference CI calculations.

Keywords: Electroabsorption spectroscopy; Poly-nuclear Ru complexes; NIR–vis spectra; Stark spectroscopy

1. Introduction

The changes of position, intensity and line-shape profile which occur when an absorbing molecule is placed in a static electric field, represent a powerful experimental technique to probe the changes in the charge distribution accompanying the transition. This technique, better known as electroabsorption (EA) spectroscopy, or Stark spectroscopy from the name of the physicist who discovered the basic effect, has become very popular in the last 15 years for the measurement of the dipole moment change which follows near IR and visible absorption in mono and poly-nuclear transition

* Tel.: +39-050-315-2453; fax: +39-050-3152-442.
E-mail address: ferretti@icqem.pi.cnr.it (A. Ferretti).

0010-8545/03/$ - see front matter © 2003 Elsevier Science B.V. All rights reserved.
doi:10.1016/S0010-8545(03)00003-1

metal complexes. Especially in this latter case, such a piece of information is indeed of basic importance, since it may be used to discuss the problem of electron localization/delocalization.

Chemical systems made by two or more metallic centers which are held together by organic molecular bridges are now widely synthesized and studied in light of the electrical [1], optical [2] and magnetic [3] properties which may arise from an efficient intramolecular electron [4] and/or energy transfer [5]. The reach of a clear understanding of the nature of the states involved in the electron transfer process, as well as the ability to measure and/or to compute the relevant quantities ruling it, are then both of basic importance in view of governing the chemistry and physics of the process itself. In this perspective, EA spectra may indeed be of valuable help.

Donor–bridge–acceptor (DBA) systems in which both donor (D) and acceptor (A) are the same transition metal complex which can be oxidized or reduced, are a specific example of poly-metallic species which are perfect candidates for the study of intramolecular electron transfer processes which can be activated chemically or electrochemically. This aspect makes this class of inorganic compounds of potential interest for the application in molecular electronic devices [1d,6]. The presence of a center of inversion for the mixed-valent species, that with the metal atoms in different oxidation states, entails the possibility that the excess electron(s) be localized on a specific molecular fragment or delocalized on the whole molecule. In these cases, Stark spectroscopy may be useful to evaluate the extent of charge localization/delocalization.

Excellent review articles have already been published on the application of EA spectroscopy to the study of transition metal complexes [7]. Often [7b,7c] the experimental results are discussed in terms of the well known two-state Mulliken–Hush [8] model and of its generalization by Cave and Newton [9], thus allowing the derivation of relevant parameters such as effective electron transfer distances and coupling. In this context, the aim of the present work is that to supplement what has already been done with a discussion on how to obtain the EA line-shape profile for mono and poly-nuclear ligand-bridged Ru complexes, taking into account electron correlation effects and the explicit role of a few selected nuclear degrees of freedom. This can be carried out by the use of suitable model Hamiltonians for extended systems, as well as by first principle approaches for the smaller oligomers. Although the models and the computational methods which will be described could be applied in principle to the whole class of poly-metallic ligand-bridged complexes, to date these have been only considered for the study of Ru-based ionic species as $(NH_3)_5Ru–L$ and $(NH_3)_5Ru–L–Ru(NH_3)_5$ (where L is a μ N-heterocycle), for which a large amount of experimental data is available.

2. Molecular parameters from EA experiments

In this section I want to summarize the basic theory of EA spectroscopy which leads to the experimental determination of the change in dipole moment and polarizability occurring in the ground-to-excited electronic transition. These results can be incorporated in the simplest quantum model, the two-state model, to obtain effective molecular parameters.

The measurement of a Stark spectrum for an ionic species is commonly done dissolving the sample in a water–glycerol mixture 50:50 vol.% which is then frozen at 77 K to form a glassy matrix. The absorption spectrum is then recorded, with and without the application of a static electric field ($\sim 10^5$ V cm^{-1}), using a polarized beam from an appropriate light source incident at a given angle with the external field: the difference between the two absorption profiles gives the desired EA spectrum. Technical details on the experimental methods, and a critical discussion on the limits which these may have, can be found in the specific literature [7a,10].

2.1. Background theory of electroabsorption

The applications of the Stark effect to the study of the difference in the charge distribution between the ground and the excited states, as given by the change in dipole moment and polarizability, are all based on the theoretical work which Liptay [11], about 30 years ago, made on the electrochromic effect (another synonym for Stark effect), in solution, in the gas phase and in molecular crystals [12]. It is much later, in the early 1990s, that the history of EA spectroscopy as applied to inorganic mono and poly-nuclear complexes begins, with the experiments by Boxer and co-workers [13] and the first theoretical approach by Reimers and Hush [14].

When a molecule, immobilized in a frozen matrix, is embedded in an electric field F [15], its absorption spectrum changes due to the dependence of the transition energy (the position of the band) and of the transition moment (the intensity of the band) on the field. Up to the second order in F, this can be summarized by the two well known equations:

$$h\Delta\nu = -\tilde{\Delta\boldsymbol{\mu}}\cdot\mathrm{F} - \frac{1}{2}\tilde{\mathbf{F}}\cdot\Delta\boldsymbol{\alpha}\cdot\mathbf{F} \quad (1)$$

$$\boldsymbol{\mu}_{ge}(\mathbf{F}) = \boldsymbol{\mu}_{ge} + \boldsymbol{\alpha}_{ge}\cdot\mathbf{F} + \frac{1}{2}\tilde{\mathbf{F}}\cdot\boldsymbol{\beta}_{ge}\cdot\mathbf{F} \quad (2)$$

In Eq. (1), h is the Planck constant, $\Delta\nu$ the frequency change, $\Delta\boldsymbol{\mu} = (\boldsymbol{\mu}_e - \boldsymbol{\mu}_g)$ and $\Delta\boldsymbol{\alpha} = (\boldsymbol{\alpha}_e - \boldsymbol{\alpha}_g)$ are the dif-

ference of dipole moment and polarizability, respectively, between the excited (e) and the ground (g) state. In Eq. (2), $\boldsymbol{\mu}_{ge}$, $\boldsymbol{\alpha}_{ge}$ and $\boldsymbol{\beta}_{ge}$ are, respectively, the transition moment, polarizability and hyperpolarizability tensors.

Taking χ as the angle between the polarization vector of the light beam and the field F, and with the assumption that $\Delta\boldsymbol{\mu}$ and $\boldsymbol{\mu}_{ge}$ are collinear (for instance along z), which is a very good approximation for the complexes considered here, the Liptay equations for the variation of the molar absorptivity ($\Delta\varepsilon(\nu)$) reduce to (see also [7,10,14]) Eqs. (3)–(6) (where the boldface for vectors and tensors variables has been substituted with their value along z):

$$\frac{\Delta\varepsilon(\nu)}{\nu} = \left[A\frac{\varepsilon(\nu)}{\nu} + \frac{B}{h}\frac{\mathrm{d}(\varepsilon(\nu)/\nu)}{\mathrm{d}\nu} + \frac{C}{2h^2}\frac{\mathrm{d}^2(\varepsilon(\nu)/\nu)}{\mathrm{d}\nu^2}\right] \times \frac{1+2\cos^2\chi}{5}F^2 \quad (3)$$

$$A = \left(\frac{\alpha_{ge}}{\mu_{ge}}\right)^2 + 2\frac{\beta_{ge}}{\mu_{ge}} \quad (4)$$

$$B = 2\frac{\alpha_{ge}\Delta\mu}{\mu_{ge}} + \frac{\Delta\alpha}{2} \quad (5)$$

$$C = (\Delta\mu)^2 \quad (6)$$

The resulting effects of the application of the field F on the spectral band are then summarized by the three terms A, B and C of Eqs. (4)–(6). The term A comes from the dependence of the transition dipole on the field (Eq. (2)) and causes an homogeneous variation in the intensity of the band. The first and the second derivative terms B and C can essentially be associated with the dependence of the position of the band on the field (Eq. (1)). C is dominated by the difference in the dipole moments of the ground and excited states and thus the presence of a large second derivative contribution in the EA spectrum can be related to a significant difference in the charge distribution between the ground and the excited state (see Fig. 1a): the observed EA line-shape will in this case be asymmetric for the first term of B (Eq. (5)). In the opposite situation, that is when the ground and the excited states involved in the transition have about the same charge distribution, $\Delta\mu$ is close to zero, and the EA spectrum will be dominated by the first derivative term with B being essentially the difference of polarization between the excited state and the ground state of Eq. (1) (Fig. 1b).

Eqs. (3)–(6) fix then the relationship between the measurement of an EA spectrum and the molecular parameters connected to the electronic charge distribution in the ground and excited states involved in the transition and to their response properties (dipole moment and polarizability). The observation of a three-lobe shaped EA line-shape profile such as that of

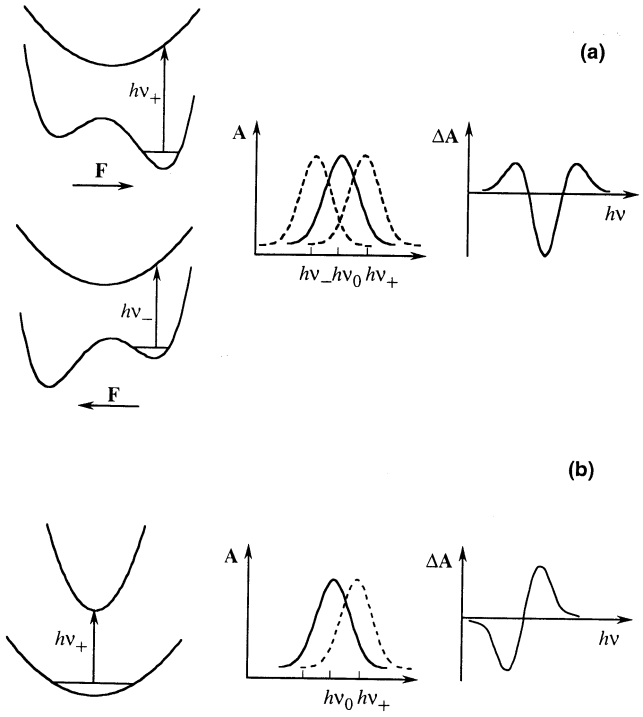

Fig. 1. One-dimensional scheme of a charge localized (a) and delocalized (b) system under the action of a static electric field F. In the localized case (a) the field breaks the symmetry of the double well: depending on the molecular orientation the zero-field spectrum (continuous line) is then displaced to higher and/or lower energy (dashed line) and the resulting EA spectrum (ΔA) has the typical positive-negative-positive three-lobe behavior. In the delocalized case (b), in the absence of a double well potential, the field causes only a blue shift of the band (due to the molecule-field interaction term) and the resulting EA spectrum then has a negative-positive two-lobe behavior.

Fig. 1a, indicates a considerable variation in the charge distribution upon excitation, and may be related to electronic charge localization. On the other hand, a two-lobe shaped profile similar to that of Fig. 1b, which is instead the signature that the ground and excited states have about the same charge distribution, may be related to charge delocalization. In principle, the application of EA spectroscopy to the well known mixed-valence complexes [7,10,13,14,16–18] can then be seen as a method capable of distinguishing between charge localized (Fig. 1a) and delocalized (Fig. 1b) species.

Bi- and poly-nuclear ligand bridged complexes having the same metal with a different oxidation number (mixed-valent species) became very popular after the work by Creutz and Taube [19] reporting on the preparation and the near IR-visible spectroscopic analysis of the +5 pyrazine-bridged bi-ruthenium ion, and research in the field is still intense [20,21] (the list is far from complete but I have tried to cite the more recent reports by each research group). The classification of the complex within the Robin–Day scheme [22] according to the localization/delocalization of the unpaired elec-

tron on a specific molecular fragment gave rise to a long debate to which a significant contribution was given by the Oh–Sano–Boxer EA experiments [13]. In spite of the conclusions drawn by EA spectroscopy pointing towards delocalization, the debate still continues [20d].

Although the aim of this review article is not that of dealing with the specific problem of localization/delocalization (see for instance Refs. [20d,23]), in this connection a remark regarding the limits of the EA experiment (see also Ref. [7a]) when applied to symmetric DBA systems should be made. Since EA spectra are recorded in a water–glycerol glass at low temperature, problems in their interpretations in terms of the charge distribution in the ground and excited molecular state may arise due to the role that solute–solvent interactions have on electron localization. These problems concern species which, from the EA spectrum, show significant variation in the dipole moment upon excitation. In fact, while a 'delocalized' system, which gives an EA line-shape profile similar to that of Fig. 1b, certainly is per se characterized by a symmetric charge distribution, the observation of 'localized' behavior such as that of Fig. 1a might be ascribed to the localizing effect of the glassy matrix. This aspect is further discussed in Section 3 where, without considering Jahn–Teller effects in detail [24], nuclear degrees of freedom and vibronic coupling are introduced. The reason for the use of inverted commas is that one can discuss delocalization or localization only relatively to a specific time scale, which in this case is that of the absorption process.

Two further problems related to the glassy matrix may exist. First, the distribution of molecular orientation may not be isotropic [23]. Second, the estimate of the effective field acting on the molecule according to dielectric continuum models [15], may be too great a simplification in the case of inorganic complexes forming hydrogen bonds with the solvent [4d,12,18f,25]. These problems have already been raised in the literature [26], in connection with the study of the effective solvent polarity of frozen solvent glasses. Although experiments performed by varying the freezing speed might be significant in the discussion of electron localization/delocalization, no specific study on inorganic complexes has been carried out to my knowledge.

2.2. Two-state electronic model

The changes in the dipole moment upon electronic excitation obtained from a fit of the experimental EA profile using Eqs. (3)–(6) (details can be found in Ref. [7]), may generate interesting interpretations when incorporated in a simple two-state electronic model describing a donor–acceptor (DA) couple. These are the essence of the Mulliken–Hush (MH) theory [8,14] in its generalization by Cave and Newton (GMH) [9]. While more detail on the theory can be found in the articles by Newton [27] (see also Ref. [28] for a very recent application of the GMH method to a three-state system), I will briefly outline here the connection between the model and EA experiments.

The two-state model is the simplest model of a system in which electron transfer occurs. The Hamiltonian and dipole matrices for the DA system are written, in the localized (or diabatic) orthonormal basis of the donor and acceptor states, as:

$$H = \begin{pmatrix} 0 & t \\ t & \Delta \end{pmatrix} \tag{7}$$

$$\mu = \begin{pmatrix} -geR & 0 \\ 0 & (1-g)eR \end{pmatrix} \tag{8}$$

where in Eq. (7) t is the DA coupling and $\Delta = \varepsilon_A - \varepsilon_D$ the energy gap between the two states and in Eq. (8) eR is the effective D–A dipole moment difference and g a factor governing the position of D and A with respect to the origin of the coordinate system placed in the center of mass (since the dipole is invariant with respect to the origin, any value of g gives the same result).

Diagonalizing the Hamiltonian of Eq. (7) and using the dipole matrix of Eq. (8), one obtains the well known results:

$$h\nu_m = E_{ge} = \sqrt{\Delta^2 + 4t^2} \tag{9}$$

$$\mu_{ge} = \frac{teR}{E_{ge}} \tag{10}$$

$$\Delta\mu = \frac{eR\Delta}{E_{ge}} \tag{11}$$

$$eR = \sqrt{(\Delta\mu)^2 + 4\mu_{ge}^2} \tag{12}$$

where $h\nu_m = E_{ge}$ is the absorption maximum.

Eqs. (9)–(12) set the relationships between quantities measurable by absorption and EA experiments, E_{ge}, μ_{ge} and $\Delta\mu$, and the parameters, t, Δ and eR of the theory: t can be associated with the rate of electron transfer between the charge-localized states D and A.

The neglect of vibronic effects [29] and the assumption that eR is the dipole moment change corresponding to the transfer of one electron across the D–A geometric separation, has made the model strictly applicable only to strongly localized systems. It has been reformulated [9], such that the effective D–A dipole moment difference is taken as an adjustable parameter [14] through comparison with the experiments or is derived by Eq. (12) using experimental or computational data for μ_{ge} and $\Delta\mu$ [9,10], thus allowing the evaluation of the effective D–A distance for one-electron transfer. This has given the method wider applicability (see e.g. Refs. [7b,7c,8–10,16,28]). The idea underlying GMH is that 'if and only if' the dipole matrix is diagonal one has strictly localized diabatic states, while this was set by construction in the early MH approach.

From Eqs. (9)–(12), localization in the DA species, which occurs when the off diagonal term t in the Hamiltonian of Eq. (7) is much smaller than the D–A energy gap ($t \ll \Delta$), causes a decrease in the intensity of the charge transfer band (proportional to $|\mu_{ge}|^2$). Correspondingly, the character of the band, in terms of the localized D and A states, becomes that of a pure D→A transition and $\Delta\mu \cong eR$ is then close to the product of a whole electronic charge with the geometric D–A separation. On the other hand, sufficiently large values of t delocalize the electronic charge and the two resulting adiabatic states, which now give rise to an intense transition, can no longer be seen in terms of the diabatic D and A states. The value of eR which is derived in these cases is generally smaller than the product of a whole electronic charge with the geometric D–A distance and attempts have been made to explain this observation [7b].

In the specific case of DBA systems, assuming that B participate with one of its empty states to the D–A charge transfer, we have to distinguish the two cases where the bridge state can or cannot be projected out by a perturbation approach. In the first situation, when the BD and BA energy gaps are much higher than D–B and B–A interactions, the system exhibit a certain degree of localization and one falls in the DA case discussed above with an effective DA coupling t_{DA} given by quasi-degenerate second order perturbation theory [30]:

$$t_{DA} = \frac{H_{DB}H_{BA}}{E_{DB}} \tag{13}$$

In this case the optical spectrum will show only a weak D–A transition. In the opposite case, the bridge state enters the problem explicitly and two bands are in general expected between the ground state and the two excited adiabatic states in which D, B and A basis (diabatic) states are differently present. Only up to moderate coupling can the two bands still be seen roughly as D→A or D→B charge transfer transitions. For strong coupling this interpretation is no longer valid and all three diabatic states (D, B and A) contribute to the three adiabatic eigenstates. This does not mean that a two state model is in principle inapplicable. In fact, in the more general case where the two bands are well separated, one may be interested in a process involving only the two lowest states which can thus be modeled as in Eq. (7). In this case the effective 'D→A' band indeed involve the bridge as implicitly present in the effective 'D' and 'A' states [28,31].

For the specific case of Ru-pentamine complexes [7b], the two-state model which can be built for the monometallic species ($Ru(NH_3)_5$–L) assuming that D is the $Ru(NH_3)_5$ and A the ligand L fragment, respectively, is then certainly consistent with the interpretations of EA data in terms of Eqs. (9)–(12). The same does not strictly hold in the case of the bimetallic species ($(Ru(NH_3)_5)_2L$), where although a two-state model can still be applied to the EA data of the near IR metal-to-metal transition, thus resulting in effective metal–metal coupling [7b], the direct correspondence with the molecular fragments which form the complex is lost.

3. EA line-shape profile by vibronic model Hamiltonians

If one wishes to calculate the entire EA line-shape profile through the difference between the absorption spectrum with and without application of the electric field, the effects of the nuclear motion, including both intramolecular vibrations and solute–solvent interactions, must explicitly be taken into account. From the theoretical and computational viewpoint, this is in general an interesting but difficult task. Large molecules have tens of internal coordinates which, directly or indirectly, may be involved in the intramolecular electron transfer processes and contribute to the profile of the corresponding charge transfer band(s): this makes a complete treatment of the full vibronic problem dimensionally unaffordable. Although attempts are now being made to work out simplified methods to partition the large set of nuclear coordinates into three groups (solvent, intramolecular bath and active) which can be differently handled [32], an ab initio approach to the computation of the profile of the charge transfer band(s) can be performed to date only with drastic simplification of the nuclear problem [18f] (see Section 4). However, in order to provide a simple description of the effects of nuclear vibrations on the line-shape of the bands for the species of interest here, one can consider a model with two single, independent, local nuclear coordinates, one on each fragment of a DA couple (Q_D and Q_A), which represent the resultant of nuclear vibrations internal to D and A, respectively, and also include interaction with the solvent. Keeping the distance DA constant and assuming the two coordinates as harmonic modes differently displaced in the D and A states, the vibronic Hamiltonian which originates from that of Eq. (7) is then:

$$H = \begin{pmatrix} \varepsilon_D + T + 1/2\, k_D(Q_D - Q_D^0)^2 + 1/2\, k_A Q_A^2 & t \\ t & \varepsilon_A + T + 1/2\, k_D Q_D^2 + 1/2\, k_A(Q_A - Q_A^0)^2 \end{pmatrix} \tag{14}$$

where $T = T_D + T_A$ is the nuclear kinetic energy term and Q_D^0 and Q_A^0 are the equilibrium position of the two oscillators in the D and A state, respectively.

The two-state-two-oscillator model of Eq. (14) is the well known Piepho–Krausz–Schatz (PKS) model [29,33], formulated with the motivation of accounting for the observed line-shape profiles of metal-to-metal charge transfer (MMCT) band of strongly coupled systems, and of general validity for DA species. The model was applied in its basic form to several complexes [29,34] and, as far as I know, was the first to be investigated for calculation of EA line-shape profiles by Ondrechen and Murga [18a,35]: details can be found in Refs. [18a,29,33,35], while extensive discussion of the role of different modes is reported in Ref. [36i] and a general spectral analysis is given in Ref. [36j]. In brief, in the simplest case in which the DA system is symmetric, that is D and A are equal ($\varepsilon_D = \varepsilon_A = \varepsilon$; $k_D = k_A = k$; $Q_D^0 = Q_A^0 = \sqrt{2}\lambda$), after the well known transformation of the coordinate system to symmetric ($q_+ = (Q_D^0 + Q_A^0)/\sqrt{2}$) and antisymmetric ($q_- = (Q_D - Q_A)/\sqrt{2}$), the symmetric coordinate has the same displacement in the two electronic states and can be eliminated. The application of a static electric field F along the D–A axis of length R, introduces a diagonal $-\mu F$ term and the field-molecule Hamiltonian which results is then (the origin is taken in the center of DA at $R/2$) (Eq. (15)):

$$H = \begin{pmatrix} \varepsilon + T_- + 1/2\, k(Q_- - \lambda)^2 + eRF/2 & t \\ t & \varepsilon + T_- + 1/2\, k(Q_- + \lambda)^2 - eRF/2 \end{pmatrix} \tag{15}$$

Depending on the value of t with respect to λ, one can have the qualitative behavior as shown in Fig. 1a or b. For small t, the adiabatic potential energy surfaces (PES; obtained diagonalizing the Hamiltonian (15) without the nuclear kinetic energy T_-) keep a double well shape in the ground state and thus a symmetric absorption band is expected and a three-lobe EA profile can be observed (Fig. 1a). On the other hand, if t is large enough, one single minimum PES is found (with different width) in both ground and excited state, resulting in a non-symmetric absorption band (not reproduced in Fig. 1b for simplicity) and in a two-lobe EA profile (Fig. 1b).

The two local vibrations considered in the model can be seen as representative of the whole set of intramolecular plus solute–solvent (or glassy matrix) vibrations. The vibronic coupling then also includes solute–solvent interactions. Therefore, in some particular cases of strong coupling, characterized by a double well ground state and an EA spectrum similar to that of Fig. 1a, that which is seen may not be intrinsic to the molecular system alone but be a consequence of the presence of the medium (see also Refs. [23,26])

Based on the PKS model (two-state vibronic), several different vibronic approaches to DA and DBA systems have been considered [36], in which the number of explicitly considered electronic states and/or nuclear degrees of freedom is changed in order to improve the model in particular species or processes. In fact, although the estimate of the effective D–A distance and interaction from a two-state model (Section 2.2) are of basic interest in molecular systems in which the occurrence of electron transfer needs to be modeled for the study of the dynamics and/or the thermodynamics of the process itself [27a], one also may be interested in building a model which is based essentially on the molecular structure. This, for instance, may be conceived so that once the modeling has been set and the relevant parameters evaluated (or estimated) for a specific molecular fragment, these can be roughly exported and used in different species where the fragment is present. There is of course no theorem to state that the pursuit of this route can be successful, but the underlying idea to simplify and parametrize the full Hamiltonian is common to all semi-empirical methods [37].

In this fashion, I now want to focus on the specific poly-nuclear complexes of the kind $[Ru(NH_3)_5–(L–Ru(NH_3)_4)_{n-}–L–Ru(NH_3)_5]^{m+}$ (for L neutral, $m = 2N_{Ru(II)} + 3N_{Ru(III)}$) with pyrazine (pyz) and 4,4′-bipyridine (bpy) as aromatic bridging ligands L, whose near IR–visible (NIR–vis) EA spectra have been investigated theoretically so far, by vibronic model calculations [18] and compared with experimental data [7,10,13].

Neglecting the hydrogen atoms of the ammonia ligands these mono- and poly-nuclear species, as the DA systems discussed above, have a principal symmetry axis (the molecular axis) such that the intense NIR–vis transitions are polarized along this axis. The action of a static electric field **F** is then limited to the component of the field along the molecular axis (at an angle θ with respect to **F**) and the field-molecule Hamiltonian is:

$$H = H_{mol} - \mu F \cos\theta \tag{16}$$

where H_{mol}, the molecular Hamiltonian, is differently modeled depending on the specific system (sections below) as the sum

$$H_{mol} = H_{el} + H_{v} + H_{el-v} \quad (17)$$

where H_{el}, H_{v} and H_{el-v} are, respectively the electronic, vibrational and vibronic terms.

Since the experiments are performed in a solid matrix where the solute molecules are randomly oriented with respect to the field, comparison with the experiment is improved quantitatively by an average over the molecular axis-field angle θ (it is assumed that $\chi = 90^{\circ}$, see Section 2.1) [18c]:

$$\langle S \rangle = \int_0^{\pi} S_{\theta} \sin^3\theta \, d\theta \quad (18)$$

where S_{θ} is the spectrum computed for the component $F \cos\theta$ of F along the molecular axis (Eq. (16)), that for zero field is normalized to the experimental spectrum [18c]. In spite of the average, the limited number of spectra S_{θ} that can reasonably be computed makes this point critical as far as a quantitative comparison with experiment is concerned.

3.1. Pyrazine-bridged systems

$[Ru(NH_3)_5–pyz]^{2+}$ and $[Ru(NH_3)_5–(pyz–Ru(NH_3)_4])_n–pyz–Ru(NH_3)_5]^{m+}$ $(m = 2n+4,\ldots,3n+6)$ complexes, may be modeled taking one orbital (or effective orbital to be more precise) for each significant metallic fragment $Ru(NH_3)_5$ (site M) and one for each ligand bridge (site L), so to have a $[M–(L–M)_n]^{m+}$-type system. According to the X_{α} calculations by Ondrechen and coworkers [38], and to those which followed [25,39], these orbitals can be assumed to be a d orbital of the metallic moiety and one of the π* for the aromatic ligand, as shown in Fig. 2.

Ru(II) and Ru(III) have $4d^6$ and $4d^5$ configurations, respectively and the bridging ligand breaks the degeneracy of t_{2g} orbitals. The d_{xz} (Fig. 2) is then the highest in energy of the Ru d's [25,38,39] and it is doubly occupied for Ru(II) or singly for Ru(III), while the ligand π* is empty. The minimal significant quantities to be considered in this simplified scheme are the orbital energies ($\varepsilon_j = \varepsilon_{pyz}$, ε_{Ru}; $\Delta = \varepsilon_{pyz} - \varepsilon_{Ru}$), the d_{xz}–π* resonance integral (t), or hopping, due to backbonding interaction, and the Coulomb repulsion (U_j, j = Ru, pyz) when two electrons occupy the same orbital. These ingredients can be incorporated in a two-band Hubbard Hamiltonian [40] (the term 'two-band' originates from the field of solid state physics and means that two different species of orbitals with a different energy are considered) modeling the electronic problem for our systems with the inclusion of some electronic correlation effects:

$$H_{el} = \sum_{j,\sigma}^{Nsite} \varepsilon_j n_{j,\sigma} + t \sum_{j,\sigma}^{Nsite-1} (a_{j,\sigma}^{+} a_{j+1,\sigma} + \text{h.c.}) + U_{Ru} \times \sum_{j}^{Ru\text{-site}} n_{j,\uparrow} n_{j,\downarrow} + U_{pyz} \sum_{j}^{pyz\text{-site}} n_{j,\uparrow} n_{j,\downarrow} \quad (19)$$

where $a_{j,\sigma}^{+}$ ($a_{j,\sigma}$) is the creation (annihilation) operator for one electron in the orbital of site j with spin σ, $n_{j,\sigma} = a_{j,\sigma}^{+} a_{j,\sigma}$ is the number operator for the spinorbital $j\sigma$, $N_{site} = N_{Ru} + N_{pyz}$ is the total number of sites, and also the number of orbitals.

In the species of interest, the orbitals of Fig. 2 differently occupied with the N_e electrons ($N_e = N_{el\uparrow} + N_{el\downarrow} = N_{Ru(III)} + 2N_{Ru(II)}$; $N_{el\uparrow}$, $N_{el\downarrow} \equiv$ total number of electron with spin up, down) give rise to a reduced electronic configurational space, where for simplicity only configurations of up and down spins which give the minimum possible value of S_z are considered. This procedure, which is correct only when the Hamiltonian does not contain terms that explicitly depend on the spin, generates an N-dimensional space with

$$N = \binom{N_{site}}{N_{el\uparrow}} \binom{N_{site}}{N_{el\downarrow}}:$$

$N = 4$ for the mononuclear Ru(II) species and $N = 9$ for all three binuclear complexes with the various Ru(II)/Ru(III) combinations.

The electronic model Hamiltonian of Eq. (19) is found per se to account for and explain the observed NIR–vis absorption of the $[Ru(NH_3)_5–(L–Ru(NH_3)_4)_{n-}–L–Ru(NH_3)_5]^{m+}$ complexes up to three metals [21m,41]. The values of the parameters, which have in general been slightly adjusted in the application to various specific cases only to improve the fit with experiment, is in the range $-0.7 < t < -1.1$, $U_{Ru} \approx \Delta \approx 5$ with $U_{Ru} \leq \Delta$ (typically $U_{Ru} = 4.62$ and $\Delta = 5.06$), $U_{pyz} = 2.5$, in eV (for a study on the effects of the various terms in the model see [41a,41b]).

In the case of the mononuclear Ru(II) complex, the basis configurations can be combined so as to eliminate the component of the triplet. According to the Hamiltonian in Eq. (19) one has then a 3×3 matrix (H_{33}) where the energies of the ground and first excited metal-to-ligand charge transfer (MLCT) states, for the above values of the parameters, (U, $\Delta > t$), can be obtained with a good approximation ($\Delta > t$) by the reduced 2×2 (H_{22}) matrix as:

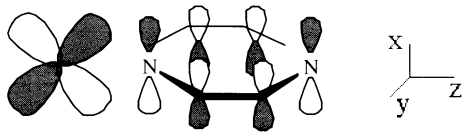

Fig. 2. Metal and ligand orbitals which are included in the simplified one-orbital-*per*-site model.

$$H_{33} = \begin{pmatrix} U_{\mathrm{Ru}} & \sqrt{2}t & \\ \sqrt{2}t & \Delta & \sqrt{2}t \\ & \sqrt{2}t & 2\Delta + U_{\mathrm{pyz}} \end{pmatrix} \Rightarrow H_{22} = \begin{pmatrix} U_{\mathrm{Ru}} & \sqrt{2}t \\ \sqrt{2}t & \Delta \end{pmatrix} \tag{20}$$

that is a reformulation of the two-state model of Eq. (7) for a DA system, also discussed in Ref. [31].

Significant nuclear degrees of freedom which may be involved in the charge transfer processes are then considered through harmonic vibrations localized on each site [36] (site vibrations), also considered in the PKS model, as well as related to local stretching modes (bond vibrations) [36d,36e,36f,36i]:

$$H_{\mathrm{v}} = \sum_{j}^{\mathrm{site}} \omega_j \left(b_j^+ b_j + \frac{1}{2} \right) + \sum_{n}^{\mathrm{bond}} \left[\omega_n^b \left(b_n^+ b_n + \frac{1}{2} \right) + \sum_{m \neq n}^{\mathrm{bond}} T_{nm} \right] \tag{21}$$

where b_j^+ (b_j), $j = \mathrm{Ru,pyz}$, and b_n^+ (b_n) are the creation (annihilation) operators for one-quantum excitation, respectively in the site oscillators of $Ru(NH_3)_5$ and pyz moieties, and in the $Ru(NH_3)_5$–pyz bond oscillators, with frequencies ω_{Ru}, ω_{pyz} and ω_n^b ($\hbar = 1$). T_{nm} is the kinetic coupling term (bond–bond) which arises transforming the kinetic energy matrix from Cartesian to local (bond) coordinates [42]; it is assumed that the nth bond is that between the n and the $n+1$ site.

In this scheme the vibronic coupling term is given by:

$$H_{\mathrm{el-v}} = \sum_{j,\sigma}^{\mathrm{site}} \lambda_j n_{j,\sigma} (b_j^+ + b_j) + \sum_{n,\sigma}^{\mathrm{bond}} \gamma_n (a_{n,\sigma}^+ a_{n+1,\sigma} + \mathrm{h.c.})(b_n^+ + b_n)] \tag{22}$$

where the two terms are the vibronic coupling for site and bond oscillators. The first is related with a displacement of the equilibrium position when the corresponding orbital is populated (see the discussion above on the PKS model) while the second term, first introduced in a different context [36e], is associated with a displacement of the bond oscillator when the electron hops between the two bound fragments. The two terms can be derived expanding the site energy (ε) and the hopping (t) of Eq. (19) on the corresponding nuclear coordinates (sites and bond) and using the general transformation:

$$q = \frac{1}{\sqrt{2m\omega}} (b + b^+) \tag{23}$$

The value of the various quantities and parameters is taken assuming that the site oscillators are roughly the symmetric Ru–NH_3 stretch of the parent $Ru(NH_3)_6$ complex and the symmetric ν_{6a} mode for the free pyz

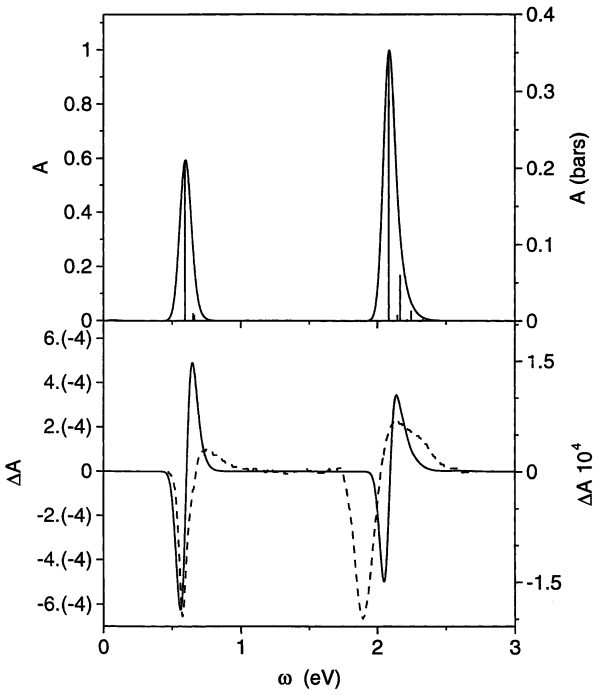

Fig. 3. Near IR–vis absorption (upper part) and electroabsorption (lower part) spectra for $[(NH_3)_5Ru\text{–}pyz\text{–}Ru(NH_3)_5]^{+5}$. The experimental EA spectrum measured in a water/glycerol glass at 77 K, taken from Ref. [13b] and shifted by −0.20 eV, is shown for comparison (dashed line, right scale). $\mathbf{F} = 4 \times 10^5$ V cm^{-1}.

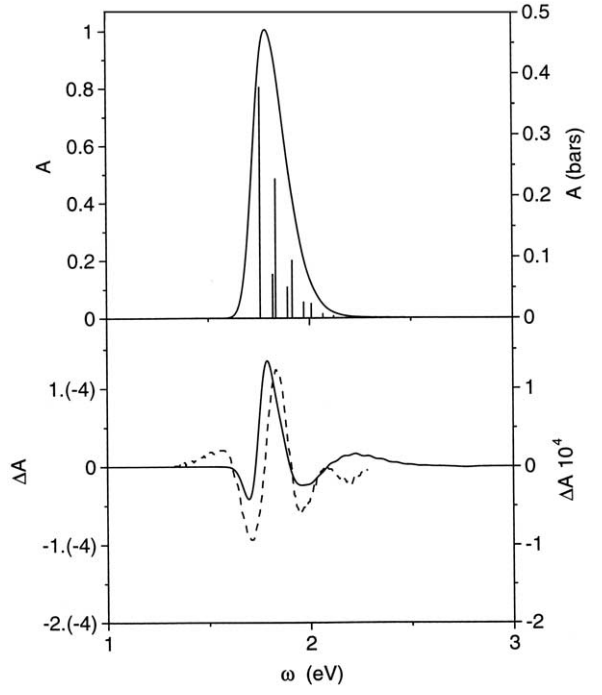

Fig. 4. Near IR–vis absorption (upper part) and electroabsorption (lower part) spectra for $[(NH_3)_5Ru\text{–}pyz\text{–}Ru(NH_3)_5]^{+4}$. The experimental EA spectrum measured in a water/glycerol glass at 77 K, taken from Ref. [13b] and shifted by −0.25 eV, is shown for comparison (dashed line, right scale). $\mathbf{F} = 4 \times 10^5$ V cm^{-1}.

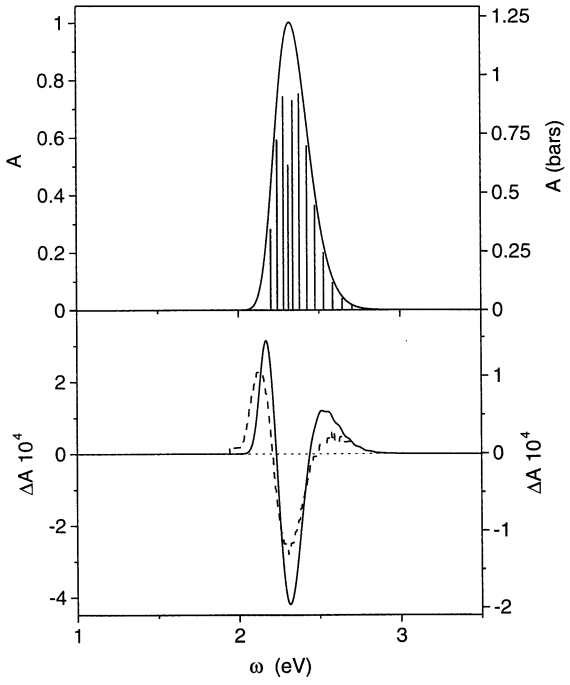

Fig. 5. $[(NH_3)_5Ru–pyz]^{+2}$ absorption (upper part) and electroabsorption (lower part) spectra computed including both site and bond oscillators. The experimental EA spectrum measured in a water/glycerol glass at 77 K, taken from Ref. [13b] and shifted by −0.15 eV, is shown for comparison (dashed line, right scale). $\mathbf{F} = 4 \times 10^5$ V cm^{-1}.

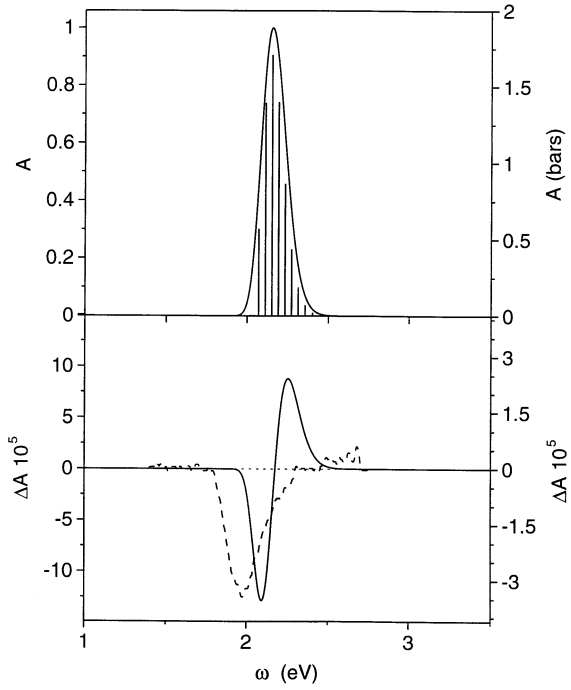

Fig. 6. $[(NH_3)_5Ru–pyz–H]^{+3}$ absorption (upper part) and electroabsorption (lower part) spectra computed including both site and bond oscillators. The experimental EA spectrum measured in a water/glycerol glass at 77 K, taken from Ref. [13b] and shifted by −0.15 eV, is shown for comparison (dashed line, right scale). $\mathbf{F} = 4 \times 10^5$ V cm^{-1}.

($\omega_{Ru} = 500$ cm^{-1}, $\omega_{pyz} = 609$ cm^{-1}; $\lambda_{Ru} = -0.1$ eV, $\lambda_{pyz} = -0.16$ eV) and the bond oscillators are the Ru–N_{pyz} stretch ($\omega_n^b = 328$ cm^{-1} and $\gamma_n = 0.023$ eV) [18c,18d,18e]. The infinite vibrational basis is made by the product of harmonic eigenfunctions, one for each oscillator, and the vibronic basis set is then built by the product with the N electronic configurations described above. Truncation of the basis in its vibrational part is then made verifying the convergence of the computed spectra.

The form of the dipole operator can be obtained by the transformation from Cartesian to internal coordinates. Taking the origin in the center of mass, one has:

$$\mu = \left(\frac{m_{Ru}}{M}\, n_{pyz} - \frac{m_{pyz}}{M}\, n_{Ru}\right)(q + q^0) \tag{24}$$

$$\mu = (q_1 + q_1^0 \quad q_2 + q_2^0) \times \begin{pmatrix} -(m_2+m_3)/M & m_1/M & m_1/M \\ -m_3/M & -m_3/M & (m_1+m_2)/M \end{pmatrix} \times \begin{pmatrix} n_1 \\ n_2 \\ n_3 \end{pmatrix} \tag{25}$$

respectively for the mono- (Eq. (24)) and bi-metallic (Eq. (25)) species; in Eq. (25) $Ru(NH_3)_5$ sites are numbered 1 and 3, pyz site is 2 (the bond coordinates q are then expressed in second quantization form using Eq. (23), q^0 are the equilibrium positions). M is the total mass.

Examples of NIR–vis EA spectra computed for the pyz systems are shown in Figs. 3–6: details of the computational technique, based on the Lanczos algorithm, can be found in Refs [18c,18d,18e,36h,41].

Although in both mixed-valent +5 (Fig. 3) and homo-valent +4 (Fig. 4) bimetallic species [18c], the bond oscillators were not included for dimensional reasons (the T_{nm} term of Eq. (21) is then absent), the computed EA line-shape profiles are in good agreement with the experiment [13b] and also account for the

Table 1
MLCT excitation energy, dipole moment, polarizability, and their variations in the MLCT for $(NH_3)_5Ru–pyz^{2+}$ and $(NH_3)_5Ru–pyz–H^{3+}$ [18e]

	$Ru–pyz^{+2}$		$Ru–pyz–H^{+3}$	
MLCT Theo (eV)	2.25		2.15	
MLCT EXP (eV)	2.49		2.33	
	Ground	Excited	Ground	Excited
μ Theo (D)	−4.91	0.670	−1.86	−1.17
$\lvert\Delta\mu\rvert$ (Debye)		5.58		0.69
$\lvert\Delta\mu\rvert$ from Exp(D)				
Ref. [13]		5.3 ± 0.8		∼0
Ref. [10]		3.5		< 2
Ref. [14]		4.93		0 ± 0.2

behavior observed in the +4 species which cannot be interpreted in terms of a two-state system (the computed absorption spectra have been scaled so to have at zero field the computed MLCT band normalized to the experimental band). This indicates that the site oscillators alone are sufficient in this case to reproduce the observed line-shape of the absorption bands. The absolute position of the computed bands is about 0.2–0.25 eV below the experimental values but their relative energy for the +5 species is reproduced well. The differences in the intensity between computed and experimental EA spectra, besides the simplicity of the model, can be explained by the limitations of the average procedure described before (Eq. (18) and discussion below). Notice that the same set of parameters is used for the two species and thus the model properly predicts both MMCT and MLCT for the +5 and the MLCT for the +4. The dipole moment in the ground and excited states is zero according to the molecular symmetry.

For the smaller monometallic complex (Fig. 5) and its protonated $[(NH_3)_5Ru–pyz\ H]^+$ analog (Fig. 6) [18e], computations can be performed including both site and bond oscillators (see Ref. [18e] for the study of the separate effect of the two kinds of vibration). The change in the permanent dipole moment which accompanies the visible region MLCT transition derived by experiment is in very good quantitative agreement with that which can be computed using the model (Table 1). Accordingly, as expected from Eq. (20), the observed change between the three-lobe profile (second derivative contribution) to the two-lobe profile (first derivative contribution) when going from the unprotonated to the protonated species, is in line here with the predictions of a two-state model (Fig. 1) with the proper choice of the band gap Δ (in eV, $\Delta = 5.36$ for the case of Fig. 5 and $\Delta = 4.62$ for that of Fig. 6).

3.2. 4,4′-Bipyridine-bridged systems

When the pyrazine is replaced by 4,4′-bipyridine (bpy), the NIR–vis EA spectra measured for the bimetallic species [13] clearly show a change in the line-shape profile from one resembling that of Fig. 1b, which occurs in a delocalized (or strongly interacting) two-state system, to that of Fig. 1a, which instead occurs in a localized (or weakly interacting) two-state system. By comparison with the +5 pyz-bridged analog, the MMCT band in the +5 bpy complex is shifted to higher energy, is more symmetric and much less intense. This matches with the prediction of a two-state charge localized system but does not explain the reasons for the occurrence of a strong MLCT band which, in the bpy species, does not differ much from that observed in the pyz systems (both for +5 and +4 ions). This is also not accounted for by the three-site model noted in the previous section (see discussion in Ref. [41c]).

With the aim of formulating a model Hamiltonian which unifies the treatment for pyz and bpy species upon oxidation/reduction as far as their NIR–vis optical properties are concerned, one may then try explicitly to consider the chemical (and topological) differences between pyz and bpy. This is translated into a reformulation of the $M–(L–M)_n$ modeling which takes into account the different bridging ligand. Since bpy is made by two pyridine (pyr) rings, it is straightforward to consider the bpy-bridged complexes as a $M–(L–L–M)_n$ system. This means that, within a one-orbital-per-site scheme, while for the $Ru(NH_3)_5$ fragment (M) one can still consider, as for the pyz-bridged species, the d_{xz} orbital (Fig. 2), in the bpy case the ligand (L–L) need to be considered as two coupled π* orbitals (each one as that of Fig. 2 for pyz). In the specific case of the bimetallic species, which is the only bpy-bridged system which has so far been theoretically and experimentally investigated, the Hubbard model Hamiltonian is then:

$$H_{\mathrm{el}} = \sum_{\sigma}[\Delta(n_{2,\sigma} + n_{3,\sigma}) + t(a^{+}_{1,\sigma}a_{2,\sigma} + a^{+}_{3,\sigma}a_{4,\sigma} + h.c.) + t'(a^{+}_{2,\sigma}a_{3,\sigma} + h.c.)]+ U_{\mathrm{Ru}}\sum_{j}^{\mathrm{Msite}} n_{j,\uparrow}n_{j,\downarrow} + U_{\mathrm{L}}\sum_{j}^{\mathrm{Lsite}} n_{j,\uparrow}n_{j,\downarrow} \quad (26)$$

where M sites are number 1 and 4, and L sites 2 and 3. The Hamiltonian of Eq. (26) basically differs from that of Eq. (19) for the t' term which represents the pyr–pyr ring coupling (L–L). The electronic configurational basis is built as for the pyz species but now one has $N = 36$ for the Ru(II)/Ru(II), $N = 24$ for the Ru(II)/Ru(III) and $N = 16$ for the Ru(III)/Ru(III) complexes. The values of the parameters are taken to be the same as those used for the pyz species and $t' \approx t/5$ [20d,41c,41d].

This model properly predict the observed NIR–vis behavior upon oxidation/reduction, although the weak band at ~1.1 eV of the +5 ion is interpreted as a MLCT transition and not as a MMCT band, which instead occurs at very small energy (~0.05 eV) [41c,41d]: the MMCT is the symmetric-to-antisymmetric (with respect to reflection) transition between states having essentially metallic character which, within the framework of the model, becomes very close in energy as localization occurs.

As far as the effects of the nuclear degrees of freedom are concerned, the same vibrational Hamiltonian of Eq. (21) with:

$$T_{nm} = -\frac{\delta_{|n-m|,1}}{m_2}\, p_n p_m; \quad p_n = i(b^{+}_{n} - b_n)\sqrt{\frac{\mu_n\omega_n}{2}} \quad (27)$$

(where μ_n is the reduced mass of the nth bond and m_2 the mass of pyr), plus the vibronic coupling Hamiltonian

of Eq. (22), have been considered. Frequencies and coupling for the pyr-site and $Ru(NH_3)_5$–pyr bonds are assumed to be the same as those for the corresponding pyz species, while for the pyr–pyr bond a frequency $\omega_2^b = 1300\ cm^{-1}$ and a coupling $\gamma_2 = -0.06$ eV have been estimated [18d].

Now the form of the dipole operator, taking into account that $m_1 = m_4$ and $m_2 = m_3$, is given by:

$$\mu = (q_1 + q_1^0 \quad q_2 + q_2^0 \quad q_3 + q_3^0) \times \begin{pmatrix} -(m_1 + 2m_2)/M & m_1/M & m_1/M & m_1/M \\ -1/2 & -1/2 & 1/2 & 1/2 \\ -m_1/M & -m_1/M & -m_1/M & (m_1 + 2m_2)/M \end{pmatrix} \times \begin{pmatrix} n_1 \\ n_2 \\ n_3 \\ n_4 \end{pmatrix} \tag{28}$$

where q_1 and q_3 are the 1–2 and 3–4 $Ru(NH_3)_5$–pyr bond coordinates, respectively, and q_2 is the pyr–pyr coordinate: all three are then transformed according to Eq. (23).

The straightforward application of the model just described to the calculation of the EA spectra for the bpy-bridged bimetallic species, however, does not provide good agreement between the computed EA lineshape profile and experiment [13]. In fact, in modeling the bpy complexes, we have taken into account only the significant degrees of freedom pertaining to the molecular systems ($Ru–NH_3$ and Ru–pyr stretch) and have not explicitly considered solute–solvent interactions.

As already discussed in Section 2.1, this may be of secondary importance for strongly interacting species such as those of the previous section, but it is more important for systems such as the bpy-bridged complexes which show the signatures of incipient localization. For such systems electron localization/delocalization may be switched on and off by changing the chemical environment, and the blockage in a solid matrix is indeed a big change [26]. This becomes clear when looking at a two-dimensional section of the eight-dimensional PES in the plane of the two anti-symmetric combinations of the coordinates on metal sites (1 and 4) and metal–ligand bonds (bonds 1 and 3 between sites 1–2 and 3–4) [18d]. This, in fact, shows a double minimum which indeed indicates the tendency towards localization, however its depth is so small that the tunneling between the two wells takes only ~ 12 ps. In this situation, the effects of introducing explicitly the effects of solute–solvent interactions may be dramatic in inducing localization. This may be simply simulated by the introduction of a small symmetry breaking term in the vibronic Hamiltonian, that is a constant difference of 5 cm^{-1} between right and left Ru and pyr sites, which, without causing a great change in the whole model, allows the convergence to a localized ground state [18d].

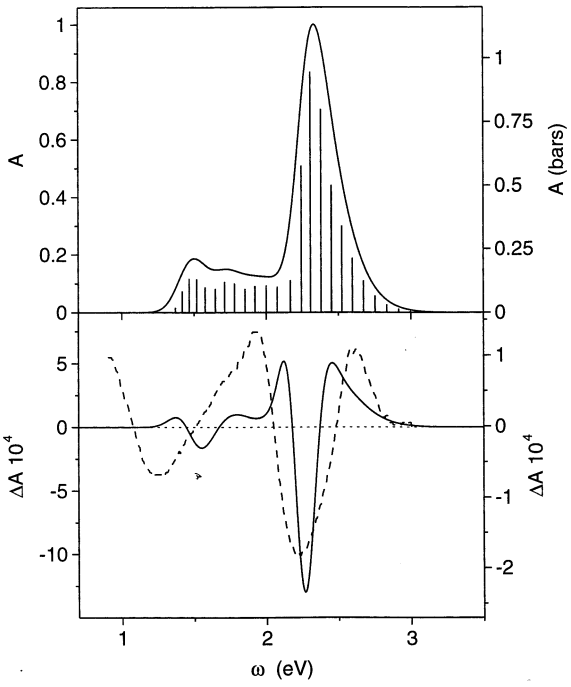

Fig. 7. Near IR–vis absorption (upper part) and electroabsorption (lower part) spectra for $[(NH_3)_5Ru–4,4'\text{-bpy}–Ru(NH_3)_5]^{+5}$ computed including only site oscillators. The experimental EA spectrum measured in a water/glycerol glass at 77 K, taken from Ref. [13b] and shifted by +0.20 eV, is reported for comparison (dashed line, right scale). $\mathbf{F} = 4 \times 10^5$ V cm^{-1}.

With the symmetry broken Hamiltonian the computed EA spectra for both +5 and +4 species become quite close to those observed experimentally (Figs. 7 and 8; as for the pyz species, the computed spectra are scaled so that the computed MLCT band is normalized to the experiment), although the agreement is not as good as in the case of the pyz-based systems. For dimensional reasons it is not possible to consider both site and bond oscillators together and this may be a possible source of difference between experiment and theory, especially for these bpy-bridged systems which are very sensitive to vibronic coupling (see Ref. [18d] for the study of the separate effect of bond and site oscillators). Another problem may be that the number and/or the type of the nuclear degrees of freedom considered in the model are insufficient to account for the observed effects. The double component of the MLCT band for the +4 species (Fig. 8), is already present in the prediction of the electronic model of Eq. (26) [41c,41d]: although the two bands of Fig. 8 do not completely merge into one in the computation, a double component of the wide MLCT transition for the +4 species was already identified by EA experiments [13b].

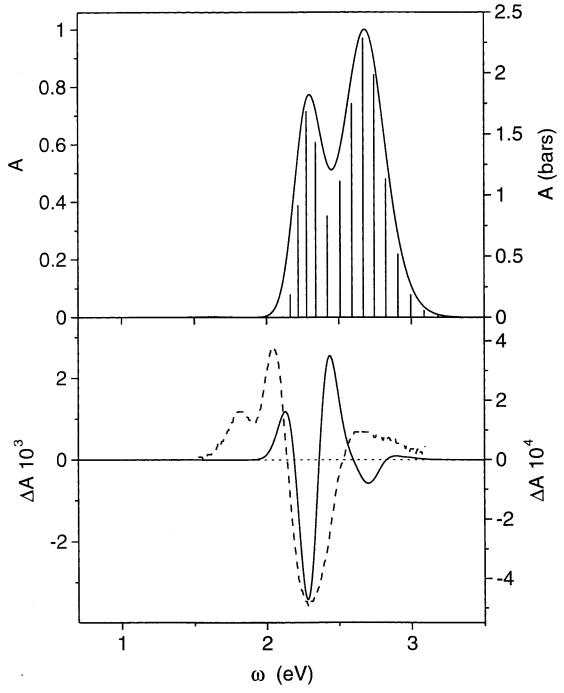

Fig. 8. Near IR–vis absorption (upper part) and electroabsorption (lower part) spectra for $[(NH_3)_5Ru–4,4'\text{-bpy}–Ru(NH_3)_5]^{+4}$ computed including only bond oscillators. The experimental EA spectrum measured in a water/glycerol glass at 77 K, taken from Ref. [13b] and shifted by +0.20 eV, is shown for comparison (dashed line, right scale). $\mathbf{F} = 4 \times 10^5$ V cm^{-1}.

4. EA spectra by ab initio calculations

The modelling of mono- and poly-nuclear metal complexes by the vibronic model Hamiltonians discussed in the previous sections allows the study of the effects of several nuclear degrees of freedom which, in more rigorous approaches may be computationally an hard task. Indeed, the complexes of interest are per se rather large and calculations which, even within the Born–Oppenheimer approximation, aim explicitly to consider the role of some nuclear degrees of freedom on the spectral properties require the construction of a multidimensional PES for the ground and the excited states of interest. Depending on the type of calculation, this can clearly be performed only for a very limited number of internal coordinates. For the specific case of the excitation spectrum in the NIR–vis of Ru complexes, several computational studies have been carried out, also with a view to investigate solvent effects [11,25,38,39,43,44], but few of them [18f,39b,39c] have explicitly considered nuclear degrees of freedom, whose effect may be rather important as far as EA spectroscopy is concerned.

An attempt to calculate the EA spectra by ab initio methods has been carried out for the binuclear homovalent Ru(II) complex $[(NH_3)_5Ru–bpy–Ru(NH_3)_5]^{+4}$ in aqueous solution [18f], first investigated by the vibronic model of the previous section [18d]. The method used [18f,25f,25g] is based on multireference configuration interaction (MRCI) calculations in which solvent effects are included by the polarizable continuum model (PCM) [45]. The only nuclear degree of freedom which has been considered is the pyr–pyr ring torsion θ, which may affect the effective metal–metal interaction.

The solute molecule is surrounded by a cavity which represents the interface with the solvent (with dielectric constant ε) which is charged by solute polarization. Since the solvents which have been so far considered may form hydrogen bonds with the metal complexes of interest (through the ammonia ligands), the cavity has been optimized to reproduce, within the framework of the PCM, the proper electron density along the H–N–Ru path (H and N of NH_3) [25f]. Notice that the PCM approach does not allow to investigate on the significant solvent–solute charge transfer which has been found in the quantum chemical study of water-complex supermolecules [25a,25b]. The charge distribution on the cavity surface generates a reaction field potential ($W(\varepsilon, \rho_a)$) which can approximately be taken the same for all the a eigenstates as that given by the charge density in the ground state (ρ_o). If H_0 is the Hamiltonian for the solute, one has then to solve:

$$(H_0 + W(\varepsilon,\ \rho_0))|\psi_a\rangle = V_a|\psi_a\rangle \tag{29}$$

The PCM–SCF–HF solution of this equation gives the best single determinant that, together with selected excited state determinants, is used in the MRCI sequence which follows [46]. This is basically carried out by few sequential steps in which the initial configuration space is each time expanded adding the contribution of its single and double excited determinants, selected by the value of their first order perturbation correction. The process ends when a satisfactory dimension of the CI space is reached [18f].

Within the Born–Oppenheimer approximation, the potential energies $V_a(\theta)$ computed by Eq. (29) at various values of the torsion, are used in the solution of:

$$\left[-\frac{1}{2I_R}\frac{d^2}{d\theta^2} + V_a(\theta)\right]\chi_{ja}(\theta) = E_{ja}\chi_{ja}(\theta) \tag{30}$$

on a basis of trigonometric functions. I_R is the reduced moment of inertia of the two rings with respect to the Ru–N–C–C–N–Ru axis, assuming free rotation of the $Ru(NH_3)_5$ fragment (hindered rotation does not affect the results).

The quantum absorption cross section is then given by:

$$\sigma_Q(\omega) = \frac{2\pi^2}{cZ_Q}\sum_{j,m} e^{-E_{j,a}/k_BT} f(m1 \leftarrow j0)\ \delta(\omega - E_{m1} + E_{j0}) \tag{31}$$

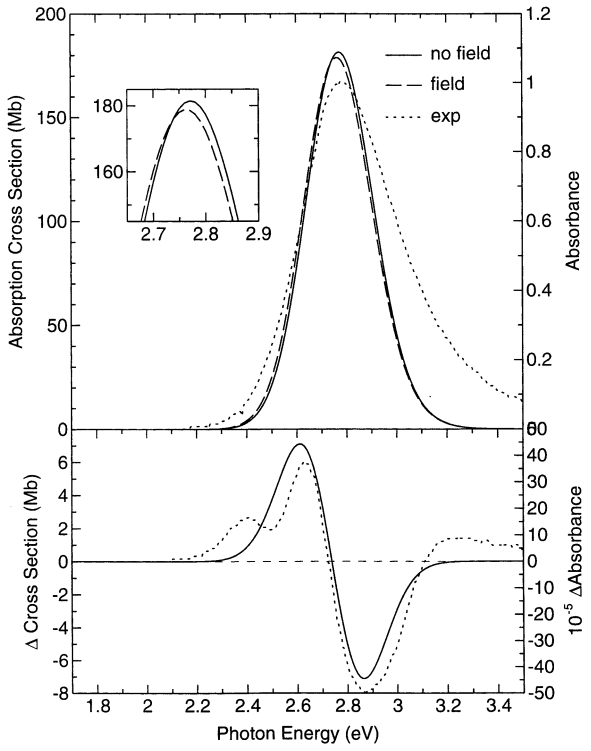

Fig. 9. Spin singlet MLCT band with and without a static electric field of 4×10^5 V cm^{-1} (upper part) and corresponding difference spectrum (lower part;1 Mb = 1×10^{-18} cm^2) for $[(NH_3)_5Ru$–4,4′-bpy–$Ru(NH_3)_5]^{+4}$ by ab initio calculations. Experimental results obtained in water/glycerol at 77 K, taken from Ref. [13b] (dotted line), are also reported for comparison and have been shifted by 0.58 eV. Reprinted with permission from Ref. [18f]. Copyright 2001 American Chemical Society.

$$f(m1 \leftarrow j0) = \frac{2}{3}(E_{m1} - E_{j0}) \left| \int \mathrm{d}\theta \chi^*_{j0}(\theta) T_{01}(\theta) \chi_{m1}(\theta) \right|^2$$

where E_{j0} and E_{m1} are the energies of the rotational states of the ground (ψ_0 and excited (ψ_1) electronic states, T_{01} the electronic transition moment between them in the dipole approximation and Z_Q is the quantum partition function of ψ_0 for the internal torsion coordinate ($Z_Q = \Sigma_j \, \mathrm{e}^{-E_{j0}/k_B T}$). The line-shape profile is obtained by the convolution with a Gaussian function with fwhm = 0.1 eV.

As before, the EA spectrum is obtained by the difference of the line-shape profile with and without the external field. It is found that the MLCT band has only one spin singlet component which alone does not explain the experimental behavior (Fig. 9). The idea that a contribution to the EA spectrum may come from the excitation to the triplet MLCT state, even if qualitatively acceptable, is not corroborated by the negligible value of the spin-orbit coupling which is computed ($\sim$ 0.5 cm^{-1}) [18f].

Attempts to carry out a similar calculation on the mixed-valent +5 bimetallic system, as well as to consider explicitly the Ru–pyr stretch vibrations, have so far failed due to the non monotonic fluctuations of the solvation energy as the coordinates change. While we hope to solve this problem soon, the results so far obtained suggest that for the bpy-bridged systems there is no definitive theoretical response with which we can be confident.

5. Conclusions

In this article I have attempted to give an overview of different theoretical approaches available for the study of EA spectra. These start with the analysis in terms of the Liptay theory that, in connection with a two-state theory, allows the derivation of molecular parameters such as the effective DA coupling and distance for the transfer of an unit electronic charge. The explicit inclusion of the effects of nuclear degrees of freedom and vibronic coupling allows the computation of the EA line-shape profile in the whole NIR–vis region of the spectrum, even for systems which are not completely described in terms of a two-state approach. This, as expected, is much more easily carried out within the framework of a molecular modeling approach, rather than by first principle methods which, however, begins to be now applicable to large systems.

I wish to conclude this article with some remarks on the future perspectives of EA spectroscopy in the field of inorganic compounds. First of all, the synthesis of polymetallic systems with various bridging ligand and the subsequent application of this technique to their study may allow us to understand several issues which still exist in the field of mixed-valence compounds, as well as in their potential application to real devices. Then, as I have tried to underline in the case of bpy-bridged species, there are systems whose NIR–vis optical properties cannot yet be clearly interpreted and where more systematic investigations may serve even basic research.

Acknowledgements

I wish to thank all the persons who have collaborated with me in this scientific adventure. Among these, I want to mention Ivo Cacelli, who, with all his patience and wisdom has introduced me to the complex and fantastic world of ab initio methods, Alessandro Lami, for all the chemistry and physics which he has been able to teach me, Mary Jo Ondrechen, for her ability to draw my attention to several aspects of mixed-valent systems, Giovanni Villani, for all the creative and heated scientific fights. Last but not least, Roberto Improta, the young and willing researcher who did most of the computations and programming for the bipyridine system. Ivo Cacelli and Alessandro Lami also have my

gratitude for the critical reading of this manuscript. I also wish to thank Paolo Palla for the help given in drawing the figures. During the revision of this article an unknown person has made a final love act donating the cornea which hopefully will give me the possibility to recover the sight in my right eye. I will never forget.

References

[1] (a) M. Hanack, S. Deger, A. Lange, Coord. Chem. Rev. 83 (1988) 11;
(b) M. Hanack, Mol. Cryst. Liq. Cryst. 160 (1988) 133;
(c) M. Hanack, M. Lang, Adv. Mater. 6 (1994) 819;
(d) A. Tomita, M. Sano, Inorg. Chem. 39 (2000) 200.

[2] (a) P.N. Prasad, D.J. Williams, Introduction to Nonlinear Optical Effects in Molecules & Polymers, John Wiley & Sons, New York, 1991;
(b) S.P. Karna, A.T. Yeates, (Eds.) Nonlinear Optical Materials: Theory and Modelling, ACS Symposium Series 628, Washington DC, 1996;
(c) S. Di Bella, Chem. Soc. Rev. 30 (2001) 355;
(d) A. Ferretti, A. Lami, G. Villani, J. Phys. Chem. 101 (1997) 9439;
(e) I.A. Sheadi, L.F. Murga, M.J. Ondrechen, J. Lindergerg, Chem. Phys. Lett. 291 (1998) 325.

[3] (a) A. Bencini, A.V. Palii, S.M. Ostrovsky, B.S. Tsukerblat, M.G. Uytterhoeven, Mol. Phys. 86 (1995) 1085;
(b) E.L. Bominaar, C. Achim, S.A. Borshch, J.J. Gired, E. Münck, Inorg. Chem. 36 (1997) 3689;
(c) V. Barone, A. Bencini, I. Ciofini, C.A. Daul, F. Totti, J. Am. Chem. Soc. 120 (1998) 8357;
(d) J.J. Borrás-Almenar, E. Coronado, S.M. Ostrovsky, A.V. Palii, B.S. Tsukerblat, Chem. Phys. Lett. 240 (1999) 149;
(e) M.I. Belinsky, Chem. Phys. Lett. 240 (1999) 303.

[4] (a) M.D. Newton, Chem. Rev. 91 (1991) 767;
(b) P.F. Barbara, T.J. Meyer, M.A. Ratner, J. Phys. Chem. 100 (1996) 13148;
(c) W.B. Davis, W.A. Svec, M.A. Ratner, M.R. Wasielewski, Nature 396 (1998) 60;
(d) P. Chen, T.J. Meyer, Chem. Rev. 98 (1998) 1439.

[5] (a) V. Balzani, F. Scandola, Supramolecular Photochemistry, Horwood, Chichester, UK, 1991;
(b) B. Schlike, P. Belser, L. De Cola, E. Sabbioni, V. Balzani, J. Am. Chem. Soc. 121 (1999) 4207;
(c) L. Flamigni, F. Barigelletti, N. Armaroli, J.P. Collin, I.M. Dixon, J.-P. Sauvage, J.A. Gareth Williams, Coord. Chem. Rev. 190–192 (1999) 671.

[6] (a) S. Woitellier, J.P. Launay, C. Joachim, Chem. Phys. 131 (1989) 481;
(b) (see papers)J. Jortner, M.A. Ratner (Eds.), Molecular Electronics, Blackwell Science, Oxford, 1997;
(c) S. Arounaguiri, B.G. Maiya, Inorg. Chem. 38 (1999) 842;
(d) F. Remacle, S. Speiser, R.D. Levine, J. Phys. Chem. Sect. B 105 (2001) 5589;
(e) Y. Asai, K. Onishi, S. Miyata, S.-J. Kim, M. Matsumoto, K. Shigehara, J. Electrochem. Soc. 148 (2001) A305.

[7] (a) G.O. Bublitz, S.G. Boxer, Annu. Rev. Phys. Chem. 48 (1997) 213;
(b) B.S. Brunschwig, C. Creutz, N. Sutin, Coord. Chem. Rev. 177 (1998) 61;
(c) F.W. Vance, R.D. Williams, J.T. Hupp, Int. Rev. Phys. Chem. 17 (1998) 307.

[8] N.S. Hush, Prog. Inorg. Chem. 8 (1967) 391.

[9] R.J. Cave, M.D. Newton, Chem. Phys. Lett. 249 (1996) 15.

[10] Y.K. Shin, B.S. Brunschwig, C. Creutz, N. Sutin, J. Phys. Chem. 100 (1996) 8157.

[11] (a) W. Liptay, Angew. Chem. Int. Ed. Engl. 8 (1969) 177;
(b) W. Liptay, in: E.C. Lim (Ed.), Excited States, vol. I, Academic Press, NY, 1974, p. 129.

[12] Solvatochromic effect, which is the dependence of position and intensity of the band on the solvent, can roughly be seen as an electrochromic effect caused by the solvent reaction field, when the solvent can be treated as a dielectric continuum medium. Unfortunately this is not the case for the present complexes. See Ref. [11b] and N.S. Hush, J.R. Reimers, Coord. Chem. Rev. 177 (1998) 37.

[13] (a) D.H. Oh, S.G. Boxer, J. Am. Chem. Soc. 112 (1990) 8161;
(b) D.H. Oh, M. Sano, S.G. Boxer, J. Am. Chem. Soc. 113 (1991) 6880.

[14] J.R. Reimers, N.S. Hush, J. Phys. Chem. 95 (1991) 9773.

[15] When a field F_{ext} is applied to the sample, the immobilized molecule feel a field $F = fF_{ext}$, where f is the local field correction. If the solute molecule is seen as in a spherical cavity surrounded by the-solvent, modeled as a dielectric continuum medium, $f = 3D/2D+1$ (D is static relative dielectric constant of the glassy matrix) and ranges between 1 and 1.3 [7c,11b,14].

[16] (a) L. Karki, H.P. Lu, J.T. Hupp, J. Phys. Chem. 100 (1996) 15637;
(b) L. Karki, J.T. Hupp, J. Am. Chem. Soc. 119 (1997) 4070;
(c) L. Karki, R.D. Williams, J.T. Hupp, Inorg. Chem. 37 (1998) 2837;
(d) F.W. Vance, L. Karki, J.K. Reigle, J.T. Hupp, M.A. Ratner, J. Phys. Chem. Sect. A 102 (1998) 8320;
(e) F.W. Vance, R.V. Slone, C.L. Stern, J.T. Hupp, Chem. Phys. 253 (2000) 313;
(f) R.C. Johnson, J.T. Hupp, J. Am. Chem. Soc. 123 (2001) 2053.

[17] (a) G.U. Bublitz, W.M. Laidlaw, R.G. Denning, S.G. Boxer, J. Am. Chem. Soc. 120 (1998) 6068;
(b) S. Franzen, V.M. Miskowski, A.P. Shreve, S.E. Wallace-Williams, W.H. Woodruff, M.R. Ondrias, M.E. Barr, L. Moore, S.G. Boxer, Inorg. Chem. 40 (2001) 6375.

[18] (a) L.F. Murga, M.J. Ondrechen, Inorg. Biochem. 70 (1998) 245;
(b) L.F. Murga, A. Ferretti, A. Lami, M.J. Ondrechen, G. Villani, Inorg. Chem. Commun. 1 (1998) 137;
(c) A. Ferretti, A. Lami, L.F. Murga, I.A. Shehadi, M.J. Ondrechen, G. Villani, J. Am. Chem. Soc. 121 (1999) 2594;
(d) A. Ferretti, A. Lami, R. Improta, G. Villani, J. Phys. Chem. 104 (2000) 201;
(e) A. Ferretti, A. Lami, R. Improta, G. Villani, Phys. Chem. Chem. Phys. 3 (2001) 2576;
(f) I. Cacelli, A. Ferretti, A. Toniolo, J. Phys. Chem. Sect. A 105 (2001) 4480.

[19] C. Creutz, H. Taube, J. Am. Chem. Soc. 91 (1969) 3988.

[20] (a) C. Creutz, Prog. Inorg. Chem. 30 (1983) 1;
(b) R.J. Crutchley, Adv. Inorg. Chem. 41 (1994) 273;
(c) J.F. Endicott, M.A. Watzky, X. Song, T. Buranda, Coord. Chem. Rev. 159 (1997) 295;
(d) K.D. Demadis, C.M. Hartshorn, T.J. Meyer, Chem. Rev. 101 (2001) 2655;
(e) J.P. Launay, Chem. Soc. Rev. 30 (2001) 386;
(f) J.T. Hupp, R.D. Williams, Acc. Chem. Res. 34 (2001) 808.

[21] (a) M.F. Hornung, F. Bauman, W. Kaim, J.A. Olabe, L.D. Slep, J. Fiedler, Inorg. Chem. 37 (1998) 311;
(b) G.N. Richardson, U. Brand, H. Vahrenkamp, Inorg. Chem. 38 (1999) 3070;
(c) M. Glöckle, W. Kaim, N.E. Katz, M.G. Posse, E.H. Cutin, J. Fiedler, Inorg. Chem. 38 (1999) 3270;
(d) Y.J. Chen, C.-H. Kao, S.J. Lin, C.-C. Tai, K.S. Kwan, Inorg. Chem. 39 (2000) 189;
(e) K.D. Demadis, G.A. Neyhart, E.M. Kober, P.S. White, T.J. Meyer, Inorg. Chem. 39 (2000) 3430;

(f) C. He, S.J. Lippard, Inorg. Chem. 39 (2000) 5225;
(g) J.F. Endicott, A.V. Macatangay, Inorg. Chem 39 (2000) 437;
(h) W. Kaim, A.L. Klein, M. Glöckle, Acc. Chem. Res. 33 (2000) 755;
(i) A. Geiss, M.J. Kolm, C. Janiak, H. Vahrenkam, Inorg. Chem. 39 (2000) 4037;
(j) P.J. Moser, G.P.A. Yap, R.J. Crutchley, Inorg. Chem. 40 (2001) 1189;
(k) M. De Rosa, C.A. White, C.E.B. Evans, R.J. Crutchley, J. Am. Chem. Soc. 123 (2001) 1396;
(l) B.W. Pfennig, V.A. Fritchman, K.A. Hayman, Inorg. Chem. 40 (2001) 255;
(m) M. Sommovigo, A. Ferretti, M. Venturi, P. Ceroni, C. Giardi, G. Denti, Inorg. Chem. 41 (2002) 1263;
(n) M. Glöckle, W. Kaim, A. Klein, E. Roduner, G. Hübner, S. Zalis, J. van Slageren, F. Renz, P. Gütlich, Inorg. Chem. 40 (2001) 2256.

[22] M.B. Robin, P. Day, Adv. Inorg. Chem. Radiochem. 10 (1967) 247.

[23] A. Lami, Chem. Phys. 273 (2001) 159.

[24] (a) I.B. Bersuker, S.A. Borshch, in: I. Prigogine, S.A. Rice (Eds.), Advances in Chemical Physics LXXXI, Wiley & Sons, New York, 1992, p. 703;
(b) I.B. Bersuker, Chem. Rev. 101 (2001) 1067.

[25] (a) K.K. Stavrev, M. Zerner, T.J. Meyer, J. Am. Chem. Soc. 117 (1995) 8684;
(b) G.M. Pearl, M. Zerner, J. Am. Chem. Soc. 121 (1999) 399;
(c) Y.K. Shin, B.S. Brunschwig, C. Creutz, M.D. Newton, N. Sutin, J. Phys. Chem. 100 (1996) 1104;
(d) J. Zeng, N.S. Hush, J.R. Reimers, J. Am. Chem. Soc. 118 (1996) 2059;
(e) J. Zeng, N.S. Hush, J.R. Reimers, J. Phys. Chem. Soc. 100 (1996) 19292;
(f) I. Cacelli, A. Ferretti, J. Chem. Phys. 109 (1998) 8583;
(g) I. Cacelli, A. Ferretti, J. Phys. Chem. 103 (1999) 4438.

[26] G.U. Bublitz, S.G. Boxer, J. Am. Chem. Soc. 120 (1998) 3988.

[27] (a) S.F. Nelsen, M.D. Newton, J. Phys. Chem. Sect. A 104 (2000) 10023;
(b) M.D. Newton, this issue of Coord. Chem. Rev.

[28] M. Rust, J. Lappe, R.J. Cave, J. Phys. Chem. A 106 (2002) 3930.

[29] (a) K.Y. Wong, P.N. Schatz, Prog. Inorg. Chem. 28 (1981) 369;
(b) R.L. Fulton, M. Gouterman, J. Chem. Phys. 41 (1964) 2280.

[30] (a) P. Durand, J.-P. Malrieu, in: K.P. Lawley (Ed.), Ab initio Methods in Quantum Chemistry—I, John Wiley & Sons, New York, 1987;
(b) M.R. Hoffmann, in: D.R Yarkony (Ed.), Modern electronic structure theory. Part. II, Advances Series in Physical Chemistry, vol. 2, World Scientific, Singapore, 1995, p. 1166.

[31] C. Creutz, M.D. Newton, N. Sutin, J. Photochem. Photobiol. A Chem. 82 (1994) 47.

[32] A. Lami, F. Santoro, J. Chem. Phys. 106 (1996) 94 (and references therein).

[33] S.B. Piepho, E.R. Krausz, P.N. Schatz, J. Am. Chem. Soc. 100 (1978) 2996.

[34] M. Tanner, A. Ludi, Inorg. Chem. 20 (1981) 2348.

[35] (a) M.J. Ondrechen, Int. Rev. Phys. Chem. 14 (1995) 1;
(b) L.F. Murga, M.J. Ondrechen, Theor. Chim. Acta 90 (1995) 331.

[36] (a) J. Ko, M.J. Ondrechen, J. Am. Chem. Soc. 107 (1985) 6161;
(b) K. Prassides, P.N. Schatz, K.Y. Wong, P. Day, J. Am. Chem. Soc. 90 (1986) 5588;
(c) M.J. Ondrechen, J. Ko, L.-T. Zhang, J. Am. Chem. Soc. 109 (1987) 1672;
(d) S.B. Piepho, J. Am. Chem. Soc. 110 (1988) 6319;
(e) R. Bozio, A. Feis, I. Zanon, C. Pecile, J. Chem. Phys. 91 (1989) 13;
(f) S.B. Piepho, J. Am. Chem. Soc. 112 (1990) 4197;
(g) K. Prassides, P.N. Schatz, Chem. Phys. Lett. 178 (1991) 227;
(h) A. Ferretti, A. Lami, M.J. Ondrechen, G. Villani, J. Phys. Chem. 99 (1995) 10484 and Erratum, 100 (1996) 20174;
(i) J.R. Reimers, N.S. Hush, Chem. Phys. 208 (1996) 177;
(j) D.S. Talaga, J.I. Zink, J. Phys. Chem. 100 (1996) 8712.

[37] (a) Frank Jensen, Introduction to Computational Chemistry, John Wiley & Sons, New York, 1999;
(b) C.H. Martin, K.F. Freed, J. Chem. Phys. 105 (1996) 1437.

[38] L.-T. Zhang, J. Ko, M.J. Ondrechen, J. Am. Chem. Soc. 109 (1987) 1666.

[39] (a) O.V. Sizova, V.I. Baranovskii, N.V. Ivanova, A.I. Panin, Russ. J. Coord. Chem. 24 (1998) 234;
(b) A. Bencini, I. Ciofini, C.A. Daul, A. Ferretti, J. Am. Chem. Soc. 121 (1999) 11418;
(c) Z. Chen, J. Bian, L. Zhang, S. Li, J. Chem. Phys. 111 (1999) 10926.

[40] J. Hubbard, Proc. R. Soc. Lond. 285 (1964) 542.

[41] (a) A. Ferretti, A. Lami, Chem. Phys. 181 (1994) 107;
(b) A. Ferretti, A. Lami, Chem. Phys. Lett. 220 (1994) 327;
(c) A. Ferretti, A. Lami, G. Villani, Inorg. Chem. 37 (1998) 2799;
(d) A. Ferretti, A. Lami, G. Villani, Inorg. Chem. 37 (1998) 4460.

[42] (a) E.B. Wilson, J.C. Decius, P.C. Cross, Molecular Vibrations, Mc Graw-Hill, New York, 1955;
(b) J.I. Steinfield, Molecules and Radiation, Harper and Row, New York, 1974.

[43] (a) S.I. Gorelsky, E.S. Dodsworth, A.B.P. Lever, A.A. Vlcek, Coord. Chem. Rev. 174 (1998) 469;
(b) A.B.P. Lever, S.I. Gorelsky, Coord. Chem. Rev. 208 (2000) 153 (and references therein).

[44] The MLCT band of the various complexes show a monotonic dependence on the solvent Gutmann donor number (V. Gutmann, *The donor–acceptor approach to molecular interactions*, Plenum, New York, 1978, p. 19) and not on the dielectric constant. In the NIR different behavior is observed depending on the bridging ligand. (a) G.M. Tom, C. Creutz, H. Taube, J. Am. Chem. Soc. 68 (1974) 7827; (b) C Creutz, M.H. Chou, Inorg. Chem. 26 (1987) 2995; (c) J.T. Hupp, T.J. Meyer, Inorg. Chem. 26 (1987) 2332.

[45] J. Tomasi, M. Persico, Chem. Rev. 94 (1994) 2027.

[46] (a) R. Cimiraglia, J. Chem. Phys. 83 (1985) 1746;
(b) C. Angeli, R. Cimiraglia, M. Persico, A. Toniolo, Theor. Chem. Acc. 98 (1997) 57.